Simplified Modeling of Masonry-Infilled RC Frames Subjected to Seismic Loads

A. Stavridis
University of Texas, Arlington

B. Shing
University of California, San Diego

15 WCEE
LISBOA 2012

SUMMARY:
This paper presents a simplified analytical method for the assessment of the seismic performance of masonry-infilled RC frames. The proposed method has been based on the results of an extended analytical and experimental study that considered non-ductile RC frames designed according to the building practice in California in the 1920s. The experimental results from a quasi-statically tested, 2/3-scale, single-story, single-bay frame have been used for the validation of a recently developed FE model which can successfully predict the behavior of these structures. The validated FE model was employed in parametric studies to explore the influence of the longitudinal and vertical reinforcement, gravity load, and frame aspect ratio. The results of the parametric studies have been used to develop a simplified analytical model. This tool can capture important features of the structural behavior such as the initial and secondary stiffness, residual strength, and provides a conservative estimate of the peak strength.

Keywords: Masonry infills, RC Frames, Simplified Modelling, Seismic Assessment, Parametric Study

1. INTRODUCTION

Evaluating the seismic performance of infilled frames has been a challenging task for structural engineers. In practice, they commonly use simplified analytical methodologies such as the diagonal strut models (ASCE 41-06 2006). Strut models have been used quite successfully (Stafford Smith 1966, Al-Chaar 2002); however, they are not accurate in representing some of the failure mechanisms exhibited by infilled frames. Moreover, the estimation of the effective strut width often relies on empirical formulas or case-specific experimental data. Hence, their usefulness as a predictive tool is limited. Alternatively, one can use limit analysis methods (Fiorato et al. 1970, Liauw and Kwan 1983, and Mehrabi et al. 1994). Nonetheless, the information they can provide is limited to the maximum resistance of the structure according to predefined failure mechanisms. Hence, their application to multi-bay, multi-story structures could be difficult due to the number of possible failure mechanisms and the possibility of not including the actual failure mechanism in the considered mechanisms.

The most powerful analysis tool is the nonlinear finite element modeling. Lotfi (1992), Lourenco (1996) and Attard et al. (2007) modeled masonry walls with a combination of continuum elements and interface elements to simulate the brick units and the mortar joints. Mehrabi and Shing (1997) simulated the behavior of masonry infilled RC frames using a combination of discrete and smeared crack elements for the RC frame and the infill panel. Their models showed some success in capturing the nonlinear behavior of the infilled frames but failed to capture some of the failure mechanisms observed in their tests. Chiou et al. (1999) modeled infilled RC frames by discretizing the brick elements and concrete members into blocks interconnected with contact springs able to simulate the tensile and shear failure.

Guidelines for the analytical assessment of infilled frames are included in ASCE 41-06. These are based on the equivalent strut approach. The guidelines, however, are not satisfactory in terms of

completeness and reliability, and have not been fully validated. The aim of this paper is to assess the influence of various parameters on the performance of these structures and to provide guidance for the development and calibration of a simplified analytical tool for the assessment of their seismic performance.

2. RC FRAME DESIGN

The frames considered in this paper are single-story, single-bay structures. They have been extracted from the external frame of the three-story prototype structure shown in Figure 1 and scaled with a length scale factor of 2/3. The prototype structure was designed to represent existing structures built in California in the 1920s. It had a non-ductile frame design and three-wythe masonry infills along the exterior frames. Details on the design of the prototype are provided by Stavridis (2009). The design of the scaled frame considered here is presented in Figure 1(b). The brick units used in all specimens were not scaled for practical reasons; therefore, the masonry walls consisted of solid clay bricks with dimensions (197 x 95 x 57 mm (7.75 x 3.75 x 2.25 in.). The head and bed joints were not scaled as well and had an average thickness of 1 cm (0.375 inches). A cement:lime:sand ratio of 1:1:5 by volume was used according to the specifications for type N mortar, which is commonly found in buildings of the 1920s era. Six frames with this frame design were tested in the University of Colorado at Boulder as part of a collaboratory project also involving researchers from Stanford University and the University of California, San Diego. The frames were studied to investigate the effect or openings and retrofit schemes using Engineered Cementitious Composite (ECC) materials. The first specimen (CU1) was the unretrofitted control specimen that had a solid infill wall. This specimen is used for the validation of the Finite Element (FE) modeling scheme employed in this study.
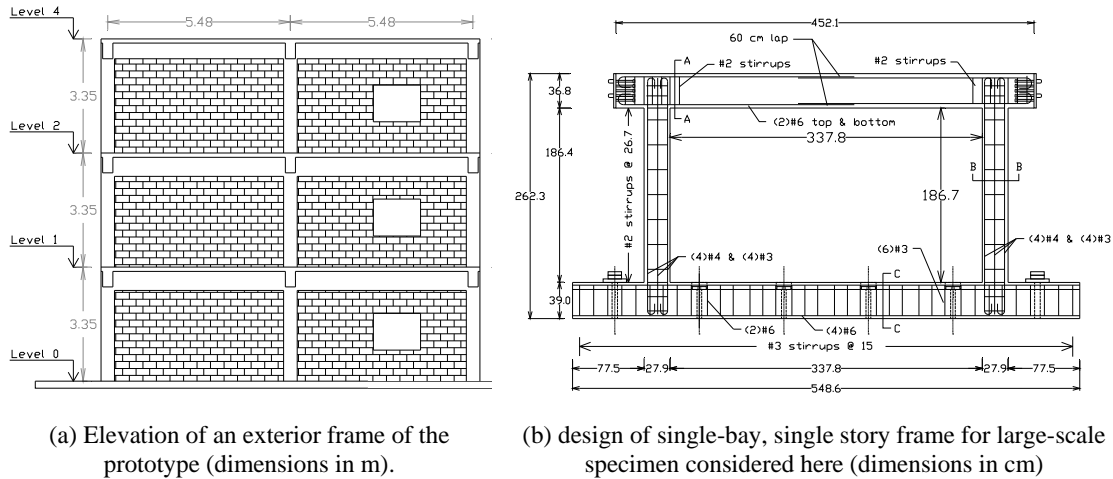

(a) Elevation of an exterior frame of the prototype (dimensions in m).

(b) design of single-bay, single story frame for large-scale specimen considered here (dimensions in cm)

Figure 1. Design of RC frame.

3. NUMERICAL MODELS

The specimen shown in Figure 1(b) was modeled with the finite element method in FEAP (Taylor 1997). The concrete columns and masonry infills are modeled with the modeling schemes developed by Stavridis and Shing (2010) which are shown in Figure 2. The foundations and beams are modeled with 4-node smeared-crack elements for computational efficiency. These members were designed to remain elastic and no discrete dominant cracks were expected. The material parameters for the finite element models have been calibrated according to the procedure developed by Stavridis and Shing (2010) based on the material tests conducted in CU (Citto 2008 and Blackard et al. 2009) and data from the literature.
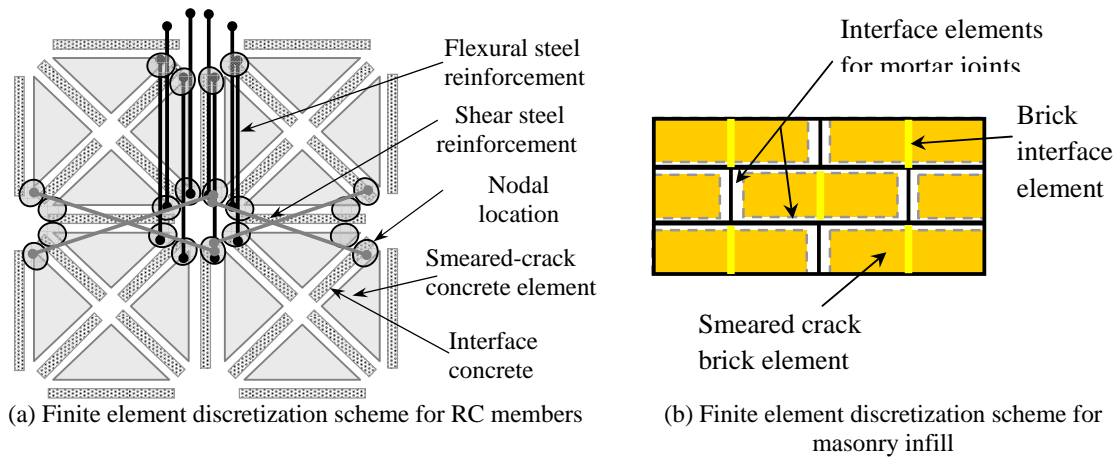
(a) Finite element discretization scheme for RC members

(b) Finite element discretization scheme for masonry infill

Figure 2. Finite element modeling schemes.

3. FE MODEL VALIDATION

The experimental load-drift relation is illustrated in Figure 3 and it is compared with the curve obtained from the finite element model. Although, the structure exhibited nonlinear behavior at a drift of 0.06% when the infill started to separate from the frame along the frame-infill interface, the lateral load continued to increase until a drift of 0.25% at which the peak resistance was reached and a dominant diagonal shear sliding crack developed in the infill. The peak strength was 685 kN (154 kips) for the positive direction of loading and 645 kN (145 kips) in the negative direction. After reaching the peak load, the specimen maintained a load capacity higher than 534 kN (120 kips) until diagonal shear cracks developed in the concrete columns as extensions of the dominant cracks in the infill. In the positive direction, a shear crack developed at the top of the windward at a drift of 0.55% and it was followed by a diagonal crack at the bottom of the leeward column at a drift of 0.75%. The same failure sequence was noted in the negative loading direction with the cracks opening at similar drift levels. After the columns failed in shear, the frame reached its residual capacity, which was 356 kN (80 kips) and it maintained that load up to 1.25% drift in both directions. A higher load was reached in the positive loading direction which was followed by a more brittle failure compared to the behavior in the negative direction as indicated by the slope of the descending branch. The test was terminated at a drift of 1.25% since the load capacity of the structure had dropped at almost 50% of the peak strength. The final cracking pattern of Specimen 1 is presented in Figure 3 and it is symmetric for the two directions of loading.

The nonlinear finite element model developed in FEAP was used to model the behavior the frame. As Figure 3(a) indicates, the model accurately captures the experimental results in terms of the initial stiffness, failure mechanism and residual strength. Figure 4(a) presents the failure mechanism of the analytical structure which accurately captures the development of the cracking pattern that leads to the failure of the specimen. The analytical prediction for the strength is 582 kN (131 kips). A shear-sliding crack initially develops in the infill and the shear cracks on the columns develop at 0.32% and 0.38% drift for the windward and the leeward column respectively. This discrepancy compared to the physical specimen can be attributed to the brittleness of the mortar joints in the analytical model. Furthermore, in the test, as the specimen deformed close to the peak value of the displacement trajectory for each cycle, the vertical load was increased at an average of 8%. This fluctuation of the vertical load could increase the lateral resistance of the specimen.

The force distribution along three cross sections of the structure at the instant of peak strength is presented in Figure 4(b). The bottom cross section is right above the shear crack at the bottom of the leeward column, while the top cross section is right below the shear crack at the top of the windward column. The third cross section is at the mid-height of the infill. For each cross section, the shear and

normal forces on the columns and the infill are shown in Figure 4. Furthermore, the forces applied on the infill from the RC frame through the frame-wall interface are also plotted.
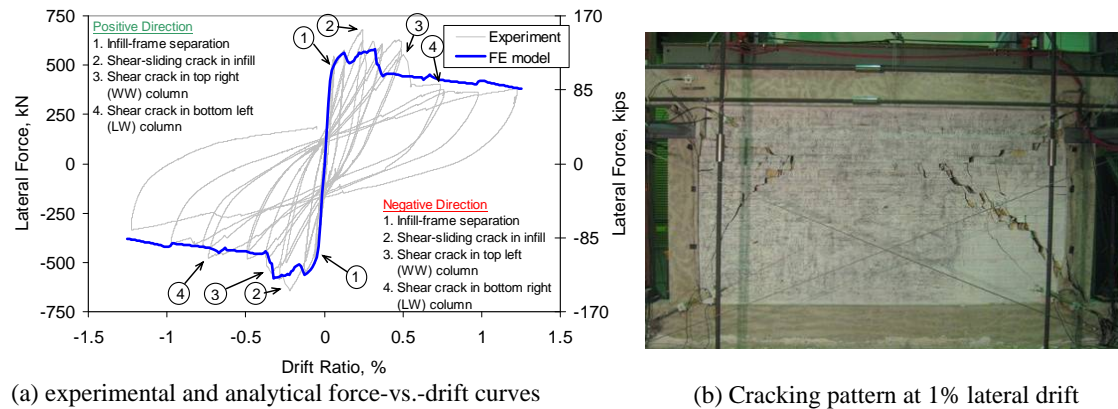

(a) experimental and analytical force-vs.-drift curves

(b) Cracking pattern at 1% lateral drift

Figure 3. Finite element modeling schemes.

As for the physical specimen, the load drops in a brittle manner due to the development of a shear crack at the top of the windward column. At this stage shear-sliding crack in the infill has fully developed and the leeward column has no shear cracks. The force distribution indicates the formation of two parallel, diagonal struts at an angle close to 45 degrees. This angle is close to the friction angle for the mortar joints. The first strut in the infill develops between the top third of the windward column and the foundation beam close to the centerline, while the second strut initiates at the top of the infill close to the centerline and ends at the bottom third of the leeward column. The force distribution changes drastically along the height of the structure, as the three cross sections indicate. At the top cross section, the windward column carries 30% of the lateral load and the infill wall carries the rest of the load. At the mid-height of the specimen, the lateral force has been transmitted to the infill and the two columns do not carry a significant portion of the vertical load, while at the bottom cross section the leeward column carries 43% of the load lateral load. After the shear cracks develop in the columns, their lateral load carrying capacity drops significantly and most of the load is carried by the infill. The strut orientation changes since the columns cannot carry lateral forces below the shear crack for the windward column and above the shear crack for the leeward column Stavridis (2009).
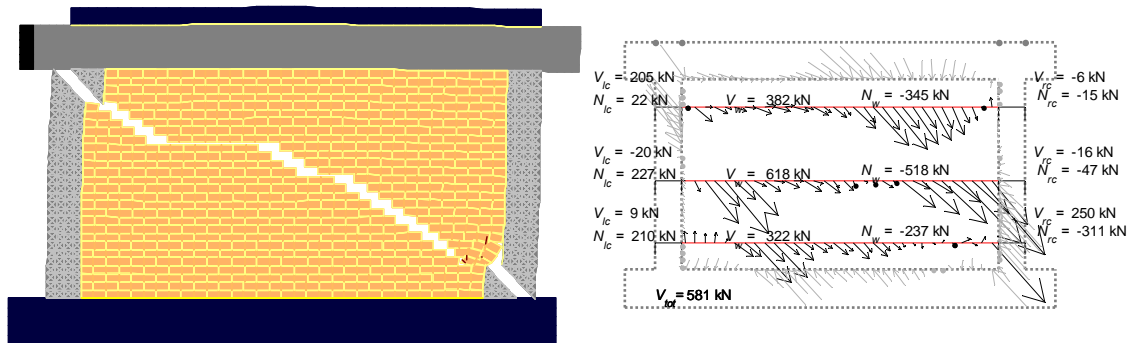

(a) failure pattern of numerical model at 1% drift

(b) force distribution along five cross sections at the instant of peak load

Figure 4. Results obtained from the analytical model.

4. PARAMETRIC STUDY

The frame studied in the previous section provided valuable insight on the behavior of an infilled RC frame under in-plane lateral loads. However, the findings from a single configuration in terms of the frame geometry, reinforcement detailing, and vertical load cannot be generalized. Hence, a parametric

study has been conducted to examine the influence of these parameters on the behavior of the RC frames with solid panels. The study has used the validated model for the CU1 specimen as a reference model and has considered four levels of vertical force, six additional aspect ratios, and four different longitudinal and four transverse reinforcing ratios for the RC columns since the reinforcing details of the beams are not expected to significantly affect the behavior of the infilled frame. The configurations considered in this study have been selected so that they allow the identification of the influence of each parameter in the structural response, rather than the represent actual cases. In all cases one parameter is varied each time to facilitate the direct comparison between different configurations and the assessment of parameter's influence. To facilitate the comparison of the results, the same material properties as for the model of specimen CU1 have been used.

The force-vs.-drift curves for the cases studied are presented in Figures 5 and 6. For conciseness, the effect of all parameters considered here is summarized in Table 1 with respect to the initial stiffness, peak strength, and failure mechanism. It is interesting to observe that the initial stiffness is only affected by the aspect ratio of the infill wall. Moreover, the strength of an infill is mostly influenced by the aspect ratio and the vertical load, which are the parameters that affect the compressive load applied on the masonry wall, the frictional resistance of which governs the overall resistance. On the other hand the amount of the longitudinal and transverse reinforcement does not influence the strength of the frame. These are important findings which can lead to the development of simplified analytical tools for the assessment of the seismic resistance of infilled frames.
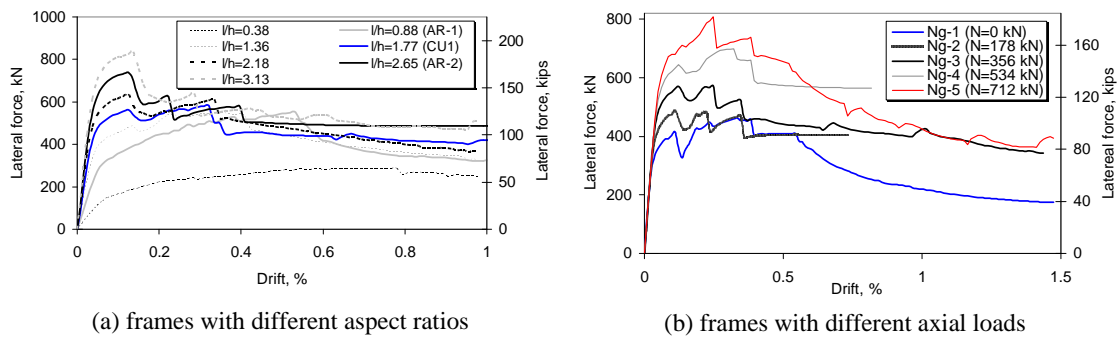

(a) frames with different aspect ratios   (b) frames with different axial loads

Figure 5. Effect of (a) aspect ratio, (b) vertical load on the load-vs.-drift curves of frames.

(a) frames with different quantities of longitudinal reinforcement   (b) frames with different quantities of transverse reinforcement
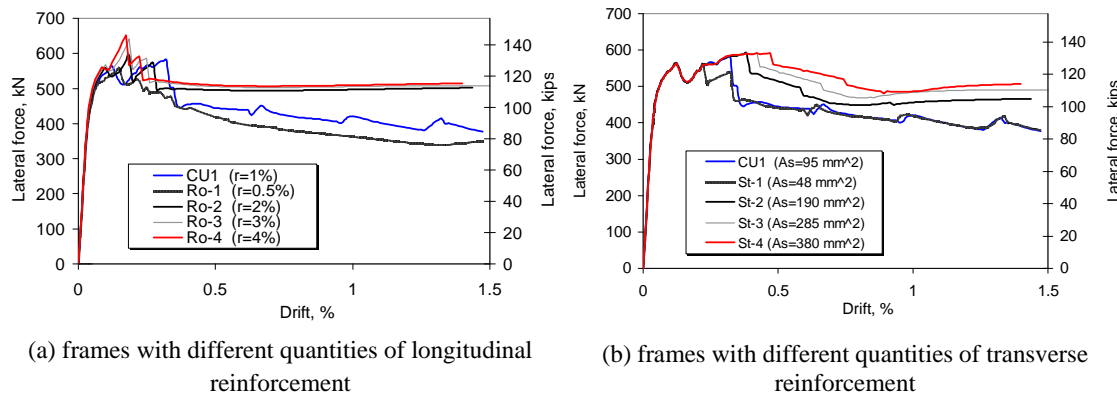
Figure 6. Effect of (a) longitudinal, (b) transverse column reinforcement on the load-vs.-drift curves of frames.

The failure mechanism of the RC columns is affected by a larger number of parameters. Especially the behavior of the windward column may change if any of the parameters considered here is altered, due to either the different axial load or the different detailing of the reinforcement. Hence the shear crack which causes a significant load drop in the case of CU1 can be delayed by increased vertical loads, and it can be prevented in the case of a larger aspect ratio or increase of the amount of shear reinforcement. Any of these changes would lead to a bending of the column and a flexural failure

mechanism as shown in Figure 7. These mechanisms are more ductile as indicated in Figures 5 and 6. On the contrary, the behavior of the leeward column does not seem to be drastically affected by the changes introduced in the design, as in all cases this column fails in shear. Although its failure mechanism does not seem to change, its strength can increase if the compressive loads increase, while a more ductile behavior can be obtained if more transverse reinforcement is used.

Table 1: Effect of design parameters on the response of RC frames with solid panels.

Parameter	Initial Stiffness	Strength	Failure Mechanism		
			Infill	Windward Column	Leeward Column
Aspect Ratio	Significant	Significant	No effect	Significant	No effect
Vertical load	No effect	Significant	No effect	Some effect	Minor effect
Ratio of Longitudinal Reinforcement	No effect	No effect	Some effect	Some effect	No effect
Area of Transverse Reinforcement	No effect	No effect	No effect	Significant	No effect
Spacing of Transverse Reinforcement	No effect	No effect	No effect	Significant	Minor effect
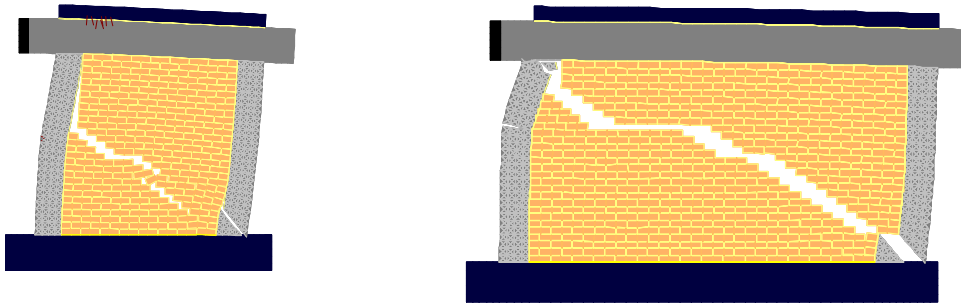
(a) model AR-1 with an aspect ratio h/L=1.10

(b) model St-2 with double transverse reinforcement in the columns compared to CU1

Figure 7. Failure patterns without shear crack in the windward column.

5. SIMPLIFIED BACKBONE CURVE FOR INFILLED FRAMES

5.1 Model Development

Based on the findings of the parametric study, a method to derive a simplified lateral force-vs.-drift behavior has been developed. The constructed curve is not an accurate representation of the actual behavior and cannot provide the amount of information on the structural performance that a detailed finite element analysis can provide. However, it is a simple yet efficient way to conservatively estimate the basic features of the structural behavior in six steps. The skeleton of the curve which is similar to that included in ASCE 41-06 is presented in Figure 8(a).

5.1.1. Step 1: Initial Stiffness, K_{ini}

The initial stiffness of an uncracked infilled frame can be calculated with the consideration of a shear beam model with the following expression proposed by used by Fiorato et al. (1970).

$$K_{ini} = \frac{1}{\dfrac{1}{K_{fl}} + \dfrac{1}{K_{shl}}} \tag{1}$$

in which K_{fl} and K_{sh} represent the flexural and shear stiffness of a cantilever column. With this approach, the structure is assumed to be a composite beam with the RC columns being the flanges and the masonry wall the web of the beam. Hence, for the flexural stiffness, K_{fl}, the equivalent properties of the composite beam should be considered, although for the shear stiffness only the contribution of the wall can be considered. The flexural stiffness can be calculated from the following expression.

$$K_{fl} = \frac{3E_c I_{ce}}{h_{cb}^3} \tag{2}$$

in which h_b is the height of the composite column measured from the top of the foundation to the mid-height of the RC beam, E_c is the modulus of elasticity of concrete, and I_{ce} is the equivalent moment of inertia of the transformed section of a transformed concrete section. I_{ce} depends on the ratio of elastic moduli of concrete and masonry and geometry of the cross-section. Alternatively, the modulus of elasticity of masonry can be used in Equation 2, if the composite cross section is transformed to an equivalent masonry cross section. Assuming that the shear stress is uniform across the wall, the shear stiffness can be calculated from the following formula.

$$K_{sh} = \frac{A_w G_w}{h_w} \tag{3}$$

in which A_w, G_w, and h_w are the cross-sectional area, shear modulus and height of the infill wall. Since the infill is not an isotropic material, its shear modulus can be either measured or calculated from empirical formulas. For instance, it can be assumed that $G_w = 0.4E_w$ (MSJC 2008), in which E_w is the modulus of elasticity of the masonry wall.
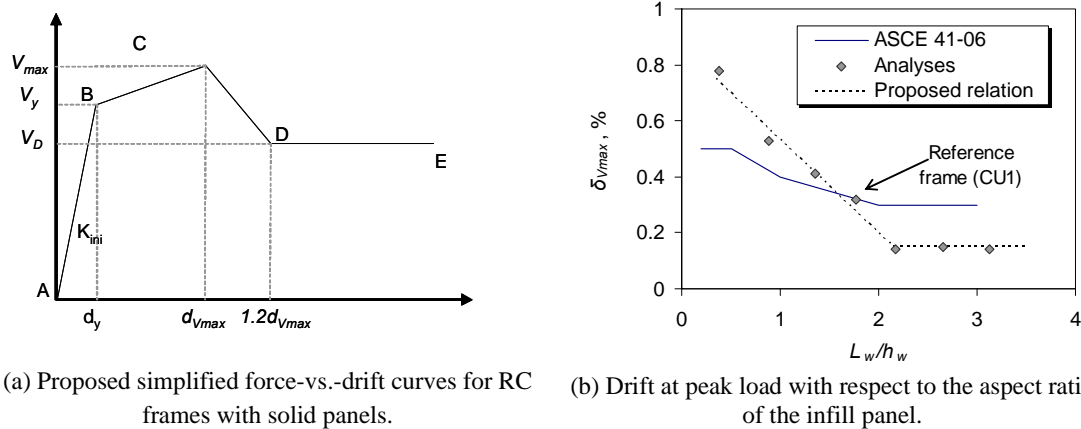

(a) Proposed simplified force-vs.-drift curves for RC frames with solid panels.

(b) Drift at peak load with respect to the aspect ratio of the infill panel.

Figure 8. Results obtained from the analytical model.

5.1.2. Step 2: Yield strength, V_y

In the cases examined in the previous sections, the yield point in the force-vs.-drift curve coincides with the separation and sliding between the infill and the RC frame. The drift and force at which the separation occurs depend on the bond quality and cohesion between the two, as well as the vertical force. The frame-infill is a statically indeterminate system and this force changes as the structure deforms. However, this study indicates that the force is in all cases between 65 and 80% of the peak

force, V_{max}, as shown by the force-vs.-displacement curves in Figures 5 and 6. Hence, a conservative estimate would be to calculate the yield force according to the following expression.

$$V_y = \frac{2}{3} V_{max} \qquad (4)$$

5.1.3. Step 3: Peak strength, V_{max}

The majority of the frames considered in this study reached the peak strength before the shear sliding crack in the infill, or prior to the shear failure of one of the columns. Knowing the failure mechanism *a priori* can help determine the strength of the structure. However, without conducting an experiment or a finite element analysis, there is no reliable tool able to predict the actual failure mechanism or strength due to the complexity of the failure mechanism. Moreover, even if the mechanism could be predicted, the distribution of vertical forces between the RC columns and the masonry wall would remain unknown as the vertical forces change along the height of the wall and columns. Therefore, a precise calculation of the peak load with a simple model is not possible. However, the peak strength of the infilled frame can be estimated based on a number of simplification assumptions.

In the method proposed here, the load on the critical cross sections of the columns is considered. These are the top cross section of the windward column and bottom cross section of the leeward column. The externally applied vertical load can be distributed on the columns and the masonry wall in proportion to their vertical stiffness. Then, a pair of vertical forces in the columns resisting the overturning moment can be considered. These forces are a function of the lateral strength of the structure and cannot be known if the lateral strength is not known. However, it can be assumed that the force in the windward column is the force required to cancel the compressive force due to the externally applied vertical load. An equal compressive force can be considered to act on the leeward column. The shear strength of the columns can be estimated based on the formulas provided by ACI 318. The total resistance of the infilled frame can be assumed to be equal to the summation of the shear resistance of the columns, the cohesion along the bed joints and the frictional force resulting from the portion of the vertical load carried by the infill.

$$V_{max} = V_{lc} + V_{rc} + c_o A_w + \mu P_w \qquad (5)$$

in which V_{lc} and V_{rc} are the shear forces carried by the columns, c_o is the cohesion strength of the mortar joints, A_w is the cross-sectional area of the infill, μ is the friction coefficient which can be assumed equal to one for an angle of 45°, and P_w is the vertical load applied on the infill.

5.1.4. Step 4: Drift at peak strength, $\delta_{V_{max}}$

The drift at peak strength cannot be easily calculated with a simplified approach as it depends on a number of parameters, including the interaction between the frame and the infill. Hence, it can be obtained from Figure 8(b) which is based on the results of the parametric study or from Table 7-9 of ASCE 41-06 (2007). This table accounts for the aspect ratio of the infill panel and the ratio of its shear strength with respect to the shear strength of the RC columns. The value of drift, $\delta_{V_{max}}$, at peak strength obtained from the table for the frames considered here would be 0.32 which is equal to the value of the CU1 model, and close to the average value of the models with the same aspect ratio considered in this study.

5.1.5. Step 5: Residual strength , V_{res}

The residual strength can be defined as the strength of the structure when a dominant shear crack has developed in the infill and propagated through the RC columns. Based on the analyses presented here, this is a worst case scenario as in some cases only one column failed due to shear. The strength of the

structure after the cracks have opened can be calculated as the summation of the residual strength of the infill due to friction along the bed joints and the residual shear resistance of the columns after the development of dominant shear cracks in both columns. In this case only the shear reinforcement crossed by a diagonal shear crack should be considered.

$$V_{res} = 2V_{c,res} + V_{w,res} \qquad (6)$$

in which $V_{c,res}$ is the residual shear strength of a column and $V_{w,res}$ is the residual shear strength of the masonry panel. The residual strength of the columns is independent of the axial load carried by each column. Moreover, for a more conservative approach this load can be assumed to be zero since the stirrups sometimes fracture at large drifts after the development of shear cracks. In the infill only the frictional resistance should be considered. The vertical load applied on the infill assumed to be equal to the externally applied load. In most of the analyses this load is higher than the externally applied load since the leeward column could not carry any load in compression after failing in shear, while the windward column is in tension to resist the overturning moment.

5.1.6. Step 6: Drift at which the residual strength is reached, $\delta_{V_{res}}$

The drift at which the residual strength is reached depends on the convention used to define the residual strength of the structure since in many cases a sudden load drop is followed by mild declining slopes. A conservative approach would be to assume a brittle load drop from the peak load to the residual strength by specifying a drift slightly larger than the drift at peak load. Based on the performance of the frames a 20% increase is proposed.

5.2. Validation of the Simplified Backbone Curve

The simplified curve proposed in the previous section has been validated with the experimental data from a small-scale tested in Stanford (Stavridis 2009) and the large-scale CU1 specimen. Figure 9 presents the comparison between the experimentally obtained curves and the curves developed with the proposed approach. In both cases, the simplified curve matches reasonably well the finite element model and the experimental results. The relatively small deviation observed around the peak load on the conservative side as the simplified prediction underestimates the strength. In terms of the residual strength, this has been calculated based on a residual friction coefficient of 0.7 and on the residual strength of the RC columns provided by the transverse reinforcement crossing an assumed shear crack on each column. Although shear cracks in the columns were not observed in the small-scale specimen, the same failure mechanism has been assumed for this frame for consistency. Finally, assuming the strut geometry proposed in the previous section, in both cases the compressive stress along the assumed diagonal struts is around 2.8 MPa (0.4 ksi), which is only a fraction of the compressive strength of masonry prisms. This low level of the stress along the compressive struts is compatible with the experimental observations concerning the lack of compressive failures in the infill panels.
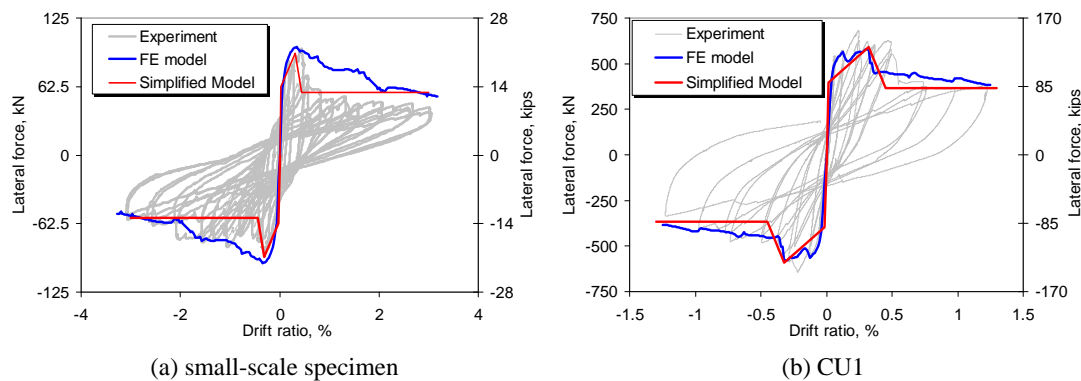

(a) small-scale specimen   (b) CU1

Figure 9. Comparison of simplified curves with experimental results.

6. CONCLUSIONS

A parametric study considering the effect of the geometry, externally applied vertical load, and reinforcement details on the performance of RC frames with solid infill walls has been conducted with the validated finite element model. The results of the study indicate that the most influential parameter is the aspect ratio of the panel as it can change the behavior of the structure drastically. The externally applied vertical load is also influential; however it does not affect the initial stiffness and its effect on the failure mechanism is only evident when its value dropped to zero, which is an extreme case. The longitudinal reinforcement has limited effect on the structural behavior, while the amount of transverse reinforcement can affect the ductility but not the strength of the structure. The results from the parametric study have been used to develop a simple procedure for the construction of a force-vs.-drift curve. The simplified model can capture important features of the structural behavior such as the initial and secondary stiffness, residual strength, and provides a conservative estimate of the peak strength. Hence, although it does not capture the failure mechanisms in detail, it provides an efficient way to obtain the basic properties of the structural performance of infilled frames.

REFERENCES

ACI 318-08 (2008). "Building Code Requirements for Structural Concrete (ACI 318-08) and Commentary." Farmington Hills, Mi.

Al-Chaar, G. (2002), "Evaluating Strength and Stiffness of Unreinforced Masonry Infill Structures." *Report No. ERDC/CERL TR-02-1*, US Army Corps of Engineers.

ASCE/SEI 41-06. (2006). "Seismic Rehabilitation of existing buildings." ASCE, New York.

Attard, M. M., A. Nappi, and F. Tin-Loi (2007). "Modeling fracture in Masonry." *J. Struct. Eng.*, ASCE, Vol. 133(10), 1385-1392.

Blackard, B., K. Willam, and S. Mettupulayam (2009). "Experimental observations of masonry infilled RC frames with openings." *ACI Special Publication SP-265*, American Concrete Institute, Farmington Hills, MI.

Chiou Y.J., J.C. Tzeng, and Y.W. Liou (1999). "Experimental and analytical study of masonry infilled frames." *J. Struct. Eng.*, ASCE, Vol. 125(10), 1109-1117.

Citto C. (2008). "Two-Dimensional Interface Model Applied to masonry structures." *Master's Thesis*. University of Colorado at Boulder.

Fiorato, A.E., M.A. Sozen, and W.L. Gamble (1970). "An investigation of the interaction of reinforced concrete frames with masonry filler walls." *Report No. UILU-ENG 70-100*, Dept. of Civ. Eng., University of Illinois at Urbana-Champaign.

Liauw T.C. and K.H Kwan (1983). "Plastic theory of infilled frames with finite interface shear strength." *Proc. Inst. Civ. Engrs*, Part 2, 1983, 75, Dec 707-723

Lotfi, H.R. (1992). "Finite element analysis of fracture of concrete and masonry structures." *Doctoral Dissertation*, University of Colorado at Boulder.

Lourenco, P.B. (1996). "Computational Strategies for masonry structures." *Doctoral Dissertation*, Delft University, Delft, The Netherlands.

Mehrabi, A.B. and P. B. Shing (1997). "Finite element modeling of masonry-infilled RC frames." *J. Struct. Eng.*, ASCE, Vol. 123(5), 604-613.

Stafford Smith, B. (1966). "Behavior of square infilled frames." *J. Struct. Div.* ASCE, 381-403.

Stavridis A. Analytical and Experimental Study of Seismic Performance of Reinforced Concrete Frames Infilled with Masonry Walls. *Ph.D. Thesis*, Univ. of California, San Diego; 2009.

Stavridis, A. and P.B. Shing. (2010). "Finite Element Modeling of Nonlinear Behavior of Masonry-Infilled RC Frames." *Journal of Structural Engineering*, *ASCE*. 136(3):285-296.

Taylor, R. L (2007). "FEAP - A Finite Element Analysis Program - Version 8.1." *Manual.* Dept. of Civil and Environmental Engineering, University of California at Berkeley, Berkeley, California.